



Title	Fabrication of fully epitaxial Co <sub>2</sub> MnSi/MgO/Co <sub>2</sub> MnSi magnetic tunnel junctions
Author(s)	Ishikawa, Takayuki; Hakamata, Shinya; Matsuda, Ken-ichi et al.
Citation	Journal of Applied Physics, 103(7), 07A919 <a href="https://doi.org/10.1063/1.2843756">https://doi.org/10.1063/1.2843756</a>
Issue Date	2008-04-01
Doc URL	<a href="https://hdl.handle.net/2115/50618">https://hdl.handle.net/2115/50618</a>
Rights	Copyright 2008 American Institute of Physics. This article may be downloaded for personal use only. Any other use requires prior permission of the author and the American Institute of Physics. The following article appeared in J. Appl. Phys. 103, 07A919 (2008) and may be found at <a href="https://dx.doi.org/10.1063/1.2843756">https://dx.doi.org/10.1063/1.2843756</a>
Type	journal article
File Information	JAP103_07A919.pdf



## Fabrication of fully epitaxial $\text{Co}_2\text{MnSi}/\text{MgO}/\text{Co}_2\text{MnSi}$ magnetic tunnel junctions

Takayuki Ishikawa,<sup>a)</sup> Shinya Hakamata, Ken-ichi Matsuda, Tetsuya Uemura, and Masafumi Yamamoto<sup>b)</sup>

*Division of Electronics for Informatics, Hokkaido University, Sapporo 060-0814, Japan*

(Presented on 6 November 2007; received 13 September 2007; accepted 22 January 2008; published online 1 April 2008)

Fully epitaxial magnetic tunnel junctions (MTJs) were fabricated with full-Heusler alloy  $\text{Co}_2\text{MnSi}$  thin films as both lower and upper electrodes and with a  $\text{MgO}$  tunnel barrier. The fabricated MTJs showed clear exchange-biased tunnel magnetoresistance (TMR) characteristics with high TMR ratios of 179% at room temperature (RT) and 683% at 4.2 K. In addition, the TMR ratio exhibited oscillations as a function of the  $\text{MgO}$  tunnel barrier thickness ( $t_{\text{MgO}}$ ) at RT, having a period of 0.28 nm, for  $t_{\text{MgO}}$  ranging from 1.8 to 3.0 nm. © 2008 American Institute of Physics.

[DOI: [10.1063/1.2843756](https://doi.org/10.1063/1.2843756)]

Highly spin-polarized electrons are essential for spintronic devices, in which both the charge and the spin of the electron are utilized as the information carrier. Half-metallic ferromagnets (HMFs) are characterized by a complete spin polarization at the Fermi level ( $E_F$ ) due to the existence of an energy gap for one spin direction (usually minority spin) (Ref. 1). The potentially high spin polarization of HMFs is widely advantageous for ferromagnetic electrodes used in spintronic devices in terms of achieving high tunnel magnetoresistance (TMR) ratios in magnetic tunnel junctions (MTJs) and efficient spin injection from ferromagnetic electrodes into semiconductors.

Co-based full-Heusler alloys ( $\text{Co}_2\text{YZ}$ ) (Ref. 2) have attracted much interest as a preferable ferromagnetic electrode material for spintronic devices. This is because of the HMF nature theoretically predicted for many of these alloys, and because of their high Curie temperatures, which are well above room temperature (RT). In particular,  $\text{Co}_2\text{MnSi}$  (CMS) has especially attracted interest because of its half-metallic nature theoretically predicted, with a large energy gap of 0.42 eV (Ref. 3) to 0.81 eV (Ref. 4). Much effort has been dedicated to fabricating and characterizing CMS thin films<sup>5–7</sup> and also to fabricating MTJs with a CMS as a lower electrode or CMS as both lower and upper electrodes and with an amorphous  $\text{AlO}_x$  barrier.<sup>8–10</sup>

We recently developed fully epitaxial MTJs with a  $\text{Co}_2\text{YZ}$  thin film [ $\text{Co}_2\text{Cr}_{0.6}\text{Fe}_{0.4}\text{Al}$  (CCFA),  $\text{Co}_2\text{MnSi}$  (CMS), or  $\text{Co}_2\text{MnGe}$  (CMG)] as a lower electrode, and a  $\text{MgO}$  (001) tunnel barrier.<sup>11–16</sup> The relatively small lattice mismatch between  $\text{Co}_2\text{YZ}$  and  $\text{MgO}$  for a  $45^\circ$  in-plane rotation (e.g., about  $-3.7\%$  for CCFA and  $-5.1\%$  for CMS) enabled us to successfully fabricate fully epitaxial MTJ trilayers featuring highly smooth and abrupt interfaces.<sup>12–15</sup> We have demonstrated relatively high TMR ratios of 109% at RT (317% at 4.2 K) for CCFA/ $\text{MgO}/\text{Co}_{50}\text{Fe}_{50}$  MTJs,<sup>14</sup> 90% at RT (192%

at 4.2 K) for CMS/ $\text{MgO}/\text{Co}_{50}\text{Fe}_{50}$  MTJs,<sup>13</sup> and 83% at RT (185% at 4.2 K) for CMG/ $\text{MgO}/\text{Co}_{50}\text{Fe}_{50}$  MTJs.<sup>16</sup> However, there is much room for further enhancement of the TMR ratio of these fully epitaxial MTJs. Since  $\text{Co}_2\text{YZ}$  thin films potentially have a high spin polarization value at RT, a promising approach would be to use these films as both the lower and upper electrodes.<sup>10,17,18</sup>

In the present study, as an extension of our work on CMS/ $\text{MgO}/\text{Co}_{50}\text{Fe}_{50}$  MTJs,<sup>13</sup> we fabricated fully epitaxial MTJs with CMS electrodes as both the lower and upper electrodes and with a  $\text{MgO}$  tunnel barrier and investigated their TMR characteristics.

We fabricated exchange-biased MTJs. In order to obtain exchange biasing, a CMS upper electrode was used in the antiferromagnetically coupled CMS/ $\text{Ru}/\text{Co}_{90}\text{Fe}_{10}$  trilayer exchange-biased through the  $\text{Co}_{90}\text{Fe}_{10}/\text{IrMn}$  interface.<sup>19</sup> The MTJ layer structure was grown on a  $\text{MgO}(001)$  single-crystal substrate and, from the substrate side, was as follows:  $\text{MgO}$  buffer (10 nm)/CMS (50 nm)/ $\text{MgO}$  barrier (0.8–3.4 nm)/CMS (5 nm)/ $\text{Ru}$  (0.8 nm)/ $\text{Co}_{90}\text{Fe}_{10}$  (2 nm)/ $\text{IrMn}$  (10 nm)/ $\text{Ru}$  cap (5 nm). Each layer in the MTJ layer structure was successively deposited in an ultrahigh vacuum chamber (base pressure of  $\sim 6 \times 10^{-8}$  Pa) using magnetron sputtering and electron beam (EB) evaporation. The CMS lower electrode was deposited by magnetron sputtering at RT and subsequently annealed *in situ* at  $600^\circ\text{C}$ , for which we have already confirmed the  $L2_1$  structure formation from x-ray pole figure measurements.<sup>7</sup> The upper CMS electrode was also deposited at RT and subsequently annealed *in situ* at up to  $600^\circ\text{C}$ . An appropriate temperature for *in situ* annealing just after the deposition of an upper CMS electrode ( $T_a$ ) is critically important for fabricating high-performance MTJs with a CMS film as the upper electrode, i.e., a higher  $T_a$  would be favorable for obtaining a high spin polarization of the upper CMS film through the improvement of structural properties,<sup>7</sup> and a  $T_a$  that does not cause the diffusion problem is also required. Given these guidelines, we fabricated CMS/ $\text{MgO}/\text{CMS}$  MTJs (hereafter, CMS-MTJs) with  $T_a$  ranging from 400 to  $600^\circ\text{C}$ .

<sup>a)</sup>Electronic mail: [ishikawa@nsed.ist.hokudai.ac.jp](mailto:ishikawa@nsed.ist.hokudai.ac.jp).

<sup>b)</sup>Author to whom correspondence should be addressed. Electronic mail: [yamamoto@nano.ist.hokudai.ac.jp](mailto:yamamoto@nano.ist.hokudai.ac.jp).

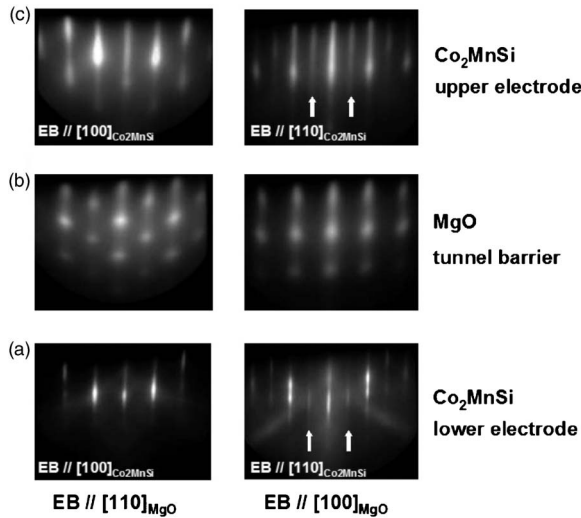


FIG. 1. RHEED patterns along the azimuths of  $[100]_{\text{MgO}}$  and  $[110]_{\text{MgO}}$  (corresponding to  $[110]_{\text{CMS}}$  and  $[100]_{\text{CMS}}$ , respectively), obtained *in situ* for each successive layer in the  $\text{Co}_2\text{MnSi}$  (CMS)/MgO/CMS trilayer structure during fabrication. (a) A lower CMS electrode deposited at RT and annealed *in situ* at  $600^\circ\text{C}$ , (b) a MgO tunnel barrier, and (c) an upper CMS electrode deposited at RT and annealed at  $500^\circ\text{C}$ . The lower and upper CMS electrodes both show additional streak patterns (indicated by arrows), showing that both had the  $L2_1$  structure.

The MgO tunnel barrier layer was deposited by EB evaporation at RT. The deposition rate was  $0.01\text{ nm/s}$  and the pressure during deposition of the MgO tunnel barrier was around  $6 \times 10^{-7}\text{ Pa}$ . The nominal thickness of the MgO tunnel barrier ( $t_{\text{MgO}}$ ) was varied from  $0.8$  to  $3.4\text{ nm}$  on each  $20 \times 20\text{ mm}^2$  substrate. The composition of the fabricated CMS film was determined to be  $\text{Co}_{2.0}\text{Mn}_{0.91}\text{Si}_{0.93}$  by inductively coupled plasma optical emission spectroscopy. We fabricated MTJs with the layer structure described above using photolithography and Ar ion milling. The fabricated junction sizes were  $8 \times 8$  and  $10 \times 10\ \mu\text{m}^2$ . We measured the TMR characteristics of the fabricated MTJs using a dc four-probe method.

Figure 1 shows RHEED patterns, along the azimuths of  $[100]_{\text{MgO}}$  and  $[110]_{\text{MgO}}$  (corresponding to  $[110]_{\text{CMS}}$  and  $[100]_{\text{CMS}}$ , respectively), observed *in situ* for each successive layer in the CMS/MgO/CMS trilayer structure during fabrication. Sharp streak patterns dependent on the electron injection direction were obtained for each successive layer in the trilayer structure, clearly indicating all the layers, including the CMS lower electrode, MgO tunnel barrier, and CMS upper electrode, grew epitaxially. We also observed  $1/2$ -order superlattice reflections along the  $[110]_{\text{CMS}}$  direction in the RHEED patterns for both the CMS lower electrode annealed at  $600^\circ\text{C}$  and the CMS upper electrode annealed at  $400$ – $600^\circ\text{C}$  [Fig. 1(c)], indicating that both had the  $L2_1$  structure.

Now, we will describe the TMR characteristics of the fully epitaxial CMS-MTJs. Figure 2(a) shows the TMR ratio at RT as a function of  $T_a$ . The bars for TMR ratios for  $T_a$  of  $550$  and  $600^\circ\text{C}$  indicate the scattering of the typical TMR ratio for each MTJ fabrication run within several runs. The TMR ratio at RT increased significantly with increasing  $T_a$  from  $80\%$  for  $T_a$  of  $400^\circ\text{C}$  to  $165 \pm 17\%$  for  $T_a$  of  $550^\circ\text{C}$ ,

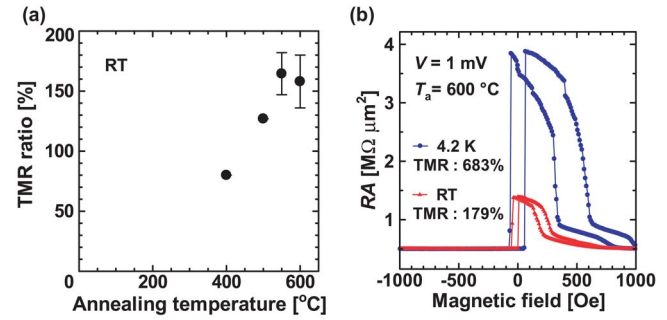


FIG. 2. (Color online) (a) TMR ratios at RT for CMS/MgO/CMS MTJs as a function of temperature for annealing just after the deposition of the CMS upper electrode ( $T_a$ ). (b) Typical tunnel magnetoresistance curves at RT and  $4.2\text{ K}$  for a CMS/MgO/CMS MTJ with  $T_a$  of  $600^\circ\text{C}$ . The junction size was  $10 \times 10\ \mu\text{m}^2$ . The bias voltage was  $1\text{ mV}$ .

and it saturated for  $T_a$  ranging from  $550$  to  $600^\circ\text{C}$ . The marked increase of the TMR ratio with increasing  $T_a$  suggests that *in situ* annealing at around  $550$  to  $600^\circ\text{C}$  considerably increased the tunneling spin polarization of the upper CMS electrode through the improvement of structural properties.

Figure 2(b) shows typical TMR curves at RT and  $4.2\text{ K}$  for a fully epitaxial CMS/MgO ( $2.1\text{ nm}$ )/CMS MTJ with  $T_a$  of  $600^\circ\text{C}$ . The junction size was  $10 \times 10\ \mu\text{m}^2$ . The bias voltage was  $1\text{ mV}$ . Clear exchange-biased TMR characteristics were obtained. The MTJ demonstrated high TMR ratios of  $179\%$  at RT and  $683\%$  at  $4.2\text{ K}$ . These values are significantly higher than the  $90\%$  at RT and  $192\%$  at  $4.2\text{ K}$  previously obtained for fully epitaxial CMS/MgO/ $\text{Co}_{50}\text{Fe}_{50}$  MTJs.<sup>13</sup> The significantly enhanced TMR ratios at both RT and  $4.2\text{ K}$  show that fully epitaxial MTJs with CMS thin films as both the lower and upper electrodes and with a MgO tunnel barrier are advantageous for obtaining high TMR ratios.

Figure 3(a) shows typical  $t_{\text{MgO}}$  dependence of  $R_p$  and  $R_{\text{AP}}$  at RT for MTJs with  $T_a$  of  $550^\circ\text{C}$  fabricated on a  $20 \times 20\text{ mm}^2$  MgO(001) substrate, where  $R_p$  and  $R_{\text{AP}}$  are the respective tunnel resistances for the parallel and antiparallel magnetization configurations between the upper and lower electrodes. The nominal junction size was  $10 \times 10\ \mu\text{m}^2$ . The bias voltage was  $5\text{ mV}$ . Both  $R_p$  and  $R_{\text{AP}}$  showed clear exponential dependence on  $t_{\text{MgO}}$  for a relatively wide  $t_{\text{MgO}}$  range from  $1.7$  to  $3.0\text{ nm}$ , indicating typical tunnel junction behavior.

Figure 3(b) shows TMR ratios as a function of  $t_{\text{MgO}}$  calculated with values of  $R_p$  and  $R_{\text{AP}}$  shown in Fig. 3(a), where the TMR ratio is defined as  $(R_{\text{AP}} - R_p)/R_p$ . The MTJs exhibited relatively high TMR ratios of over  $110\%$  at RT for a wide  $t_{\text{MgO}}$  range from  $1.8$  to  $3.0\text{ nm}$ , and the TMR ratio gradually increased from  $112\%$  to  $147\%$  for this  $t_{\text{MgO}}$  range. The TMR ratio versus  $t_{\text{MgO}}$  shown in Fig. 3(b) suggests oscillations of the TMR ratio as a function of  $t_{\text{MgO}}$  for  $t_{\text{MgO}}$  ranging from  $1.8$  to  $3.0\text{ nm}$ . In Fig. 3(b), a fitting line for the TMR ratio versus  $t_{\text{MgO}}$  with a single period of  $0.28\text{ nm}$  is plotted as a guide, and the  $t_{\text{MgO}}$  dependence of the TMR ratio is relatively well represented by this fitting curve. The oscillation period of  $0.28\text{ nm}$  is close to the oscillation period of  $0.32\text{ nm}$  for the oscillatory  $t_{\text{MgO}}$  dependence of  $R_p$  and  $R_{\text{AP}}$

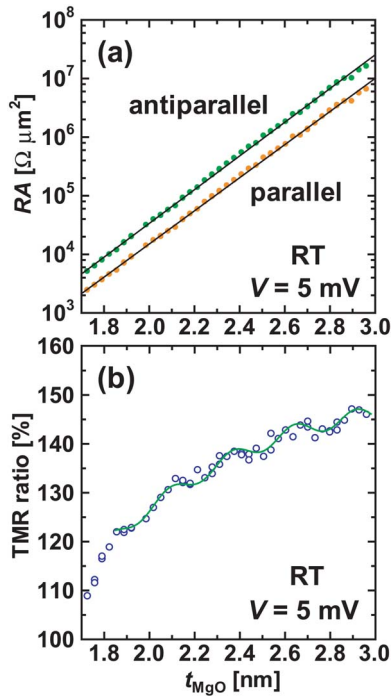


FIG. 3. (Color online) (a) Typical  $t_{\text{MgO}}$  dependence of  $R_p$  and  $R_{\text{AP}}$  at RT for CMS/MgO/CMS MTJs with  $T_d$  of 550 °C fabricated on a  $20 \times 20 \text{ nm}^2$  MgO(001) substrate, where  $R_p$  and  $R_{\text{AP}}$  are the respective tunnel resistances for the parallel and antiparallel magnetization configurations between the upper and lower electrodes. The nominal junction size was  $10 \times 10 \text{ nm}^2$ . The bias voltage was 5 mV. (b) TMR ratios as a function of  $t_{\text{MgO}}$  calculated with values of  $R_p$  and  $R_{\text{AP}}$  shown in (a), where the TMR ratio is defined as  $(R_{\text{AP}} - R_p)/R_p$ .

observed for fully epitaxial Fe/MgO/Fe MTJs.<sup>20,21</sup> We could not extract the oscillatory components of  $R_p$  and  $R_{\text{AP}}$  for the fabricated CMS-MTJs. To observe possible oscillations of  $R_p$  and  $R_{\text{AP}}$  as a function of  $t_{\text{MgO}}$ , the degree of the junction area scattering should be lower than the amplitudes of the oscillatory components of  $R_p$  and  $R_{\text{AP}}$ . But this condition was probably not satisfied in the fabricated MTJs. (The MTJ junction size was defined with photolithography.) On the other hand, the junction area scattering does not affect the TMR ratio because that the TMR ratio calculated as  $R_{\text{AP}}/R_p - 1$  is a quantity independent of the junction area. Thus, the observation of oscillations of the TMR ratio as a function of  $t_{\text{MgO}}$  is easier than that of oscillations of  $R_p$  and  $R_{\text{AP}}$ . To clarify the mechanisms of the observed oscillatory dependence of the TMR ratio, further systematic study for fully epitaxial MTJs with Heusler alloy electrodes and a MgO barrier is needed.

Finally, we will discuss possible reasons for the enhancement of the TMR ratios of the presented MTJs with CMS electrodes and with a single-crystalline MgO barrier compared with previously reported MTJs with a CMS electrode or CMS electrodes and with an amorphous  $\text{AlO}_x$  barrier.<sup>8-10</sup> First, our approach of growing fully epitaxial MTJ layer structures enables the growth of single-crystalline lower and upper  $\text{Co}_2\text{YZ}$  electrodes. Then, the high-quality single-crystalline  $\text{Co}_2\text{YZ}$  electrodes would lead to a high spin polarization of each ferromagnetic electrode. Second, fully epitaxial MTJ layer structures are advantageous for forming atomically flat and abrupt interfaces in MTJ trilayers. As a

result, the high spin polarization of potentially half-metallic CMS thin films is retained at the interfaces. Third, the combination of single-crystalline  $\text{Co}_2\text{YZ}$  thin films as lower and upper electrodes with a single-crystalline MgO tunnel barrier enables the enhancement of the tunneling spin polarization due to preferential tunneling of electrons with  $\Delta_1$  symmetry.<sup>22-24</sup> Fourth, depositing MgO barriers by EB evaporation in a ultrahigh vacuum chamber ensures that the interfacial region of CMS lower electrodes with a MgO barrier is not oxidized, which has been demonstrated directly by x-ray absorption spectroscopy and x-ray magnetic circular dichroism.<sup>25</sup>

In summary, we fabricated fully epitaxial MTJs with full-Heusler alloy CMS thin films as both lower and upper electrodes and with a MgO tunnel barrier. The fabricated MTJs demonstrated high TMR ratios of 179% at RT and 683% at 4.2 K. The demonstrated high TMR ratios confirm the promise of a single-crystalline CMS film with a combination of a single-crystalline MgO tunnel barrier as ferromagnetic electrodes in spintronic devices.

<sup>1</sup>R. A. de Groot, F. M. Mueller, P. G. van Engen, and K. H. J. Buschow, *Phys. Rev. Lett.* **50**, 2024 (1983).

<sup>2</sup>F. Heusler, *Verh. Dtsch. Phys. Ges.* **12**, 219 (1903).

<sup>3</sup>S. Ishida, S. Fujii, S. Kashiwagi, and S. Asano, *J. Phys. Soc. Jpn.* **64**, 2152 (1995).

<sup>4</sup>S. Picozzi, A. Continenza, and A. J. Freeman, *Phys. Rev. B* **66**, 094421 (2002).

<sup>5</sup>M. P. Raphael, B. Ravel, M. A. Willard, S. F. Cheng, B. N. Das, R. M. Stroud, K. M. Bussmann, J. H. Claassen, and V. G. Harris, *Appl. Phys. Lett.* **79**, 4396 (2001).

<sup>6</sup>U. Geiersbach, A. Bergmann, and K. Westerholt, *J. Magn. Magn. Mater.* **240**, 546 (2002).

<sup>7</sup>H. Kijima, T. Ishikawa, T. Marukame, H. Koyama, K.-i. Matsuda, T. Uemura, and M. Yamamoto, *IEEE Trans. Magn.* **42**, 2688 (2006).

<sup>8</sup>S. Kämmerer, A. Thomas, A. Hütten, and G. Reiss, *Appl. Phys. Lett.* **85**, 79 (2004).

<sup>9</sup>A. Hütten, J. Schmalhorst, A. Thomas, S. Kämmerer, M. Sacher, D. Ebke, N.-N. Liu, X. Kou, and G. Reiss, *J. Alloys Compd.* **423**, 148 (2006).

<sup>10</sup>Y. Sakuraba, M. Hattori, M. Oogane, Y. Ando, H. Kato, A. Sakuma, T. Miyazaki, and H. Kubota, *Appl. Phys. Lett.* **88**, 192508 (2006).

<sup>11</sup>T. Marukame, T. Kasahara, K.-i. Matsuda, T. Uemura, and M. Yamamoto, *Jpn. J. Appl. Phys., Part 2* **44**, L521 (2005).

<sup>12</sup>M. Yamamoto, T. Marukame, T. Ishikawa, K.-i. Matsuda, T. Uemura, and M. Arita, *J. Phys. D* **39**, 824 (2006).

<sup>13</sup>T. Ishikawa, T. Marukame, H. Kijima, K.-i. Matsuda, T. Uemura, M. Arita, and M. Yamamoto, *Appl. Phys. Lett.* **89**, 192505 (2006).

<sup>14</sup>T. Marukame, T. Ishikawa, S. Hakamata, K.-i. Matsuda, T. Uemura, and M. Yamamoto, *Appl. Phys. Lett.* **90**, 012508 (2007).

<sup>15</sup>T. Marukame and M. Yamamoto, *J. Appl. Phys.* **101**, 083906 (2007).

<sup>16</sup>S. Hakamata, T. Ishikawa, T. Marukame, K.-i. Matsuda, T. Uemura, M. Arita, and M. Yamamoto, *J. Appl. Phys.* **101**, 09J513 (2007).

<sup>17</sup>N. Tezuka, N. Ikeda, S. Sugimoto, and K. Inomata, *Jpn. J. Appl. Phys., Part 2* **46**, L454 (2007).

<sup>18</sup>T. Marukame, T. Ishikawa, S. Hakamata, K.-i. Matsuda, T. Uemura, and M. Yamamoto, *IEEE Trans. Magn.* **43**, 2782 (2007).

<sup>19</sup>T. Ishikawa, T. Marukame, K.-i. Matsuda, T. Uemura, and M. Yamamoto, *IEEE Trans. Magn.* **42**, 3002 (2006).

<sup>20</sup>S. Yuasa, T. Nagahama, A. Fukushima, Y. Suzuki, and K. Ando, *Nat. Mater.* **3**, 868 (2004).

<sup>21</sup>R. Matsumoto, A. Fukushima, T. Nagahama, Y. Suzuki, K. Ando, and S. Yuasa, *Appl. Phys. Lett.* **90**, 252506 (2007).

<sup>22</sup>W. H. Butler, X.-G. Zhang, T. C. Schulthess, and J. M. Maclaren, *Phys. Rev. B* **63**, 054416 (2001).

<sup>23</sup>J. Mathon and A. Umersky, *Phys. Rev. B* **63**, 220403R (2001).

<sup>24</sup>Y. Miura, H. Uchida, T. Oba, K. Nagao, and M. Shirai, *J. Phys.: Condens. Matter* **19**, 365228 (2007).

<sup>25</sup>T. Saito, T. Katayama, T. Ishikawa, M. Yamamoto, D. Asakura, and T. Koide, *Appl. Phys. Lett.* **91**, 262502 (2007).